*Article*

# Rapidly Curing Chitosan Calcium Phosphate Composites as Dental Pulp Capping Agents

**Matthew J. Osmond, Rachel R. Mizenko, Melissa D. Krebs ***

Chemical & Biological Engineering, Colorado School of Mines, 1613 Illinois Street, Golden, CO 80401, USA

**\*** Correspondence: Melissa D. Krebs, Email: mdkrebs@mines.edu;
Tel.: +1-303-273-3983.

## ABSTRACT

*Background*: Dental caries are the most prevalent yet preventable disease in both children and adults. Current treatments cannot adequately restore tooth function while concurrently supporting the regeneration of dentin tissue. The materials presented here were designed to create a rapid curing, mechanically stable and biocompatible pulp capping agent.

*Methods*: In this study, a rapidly curing dental composite was formed using carboxymethyl-chitosan, hydroxyapatite whiskers, and a diglycidyl ether. Properties of the composites that were measured include gelation, mechanical properties, and surface characteristics. Human dental pulp stem cells were cultured on the composites to determine cytocompatibility, proliferation, and differentiation potential.

*Results*: All composite components were verified using XRD and ATR-FTIR. The compressive modulus was determined to be greater than 600 kPa, swelling less than 2%, and degradation less than 10%. Composites supported the growth of cells for 3 weeks. qPCR was used to measure the pre-odontoblastic marker, RUNX2. The expression of osteocalcin was measured with confocal microscopy, which showed the differentiation to odontoblastic cells.

*Conclusions*: These materials meet the initial goals for a regenerative pulp capping agent. Further investigation could lead to the next generation of pulp capping and dental filling materials.

**KEYWORDS:** carboxymethyl chitosan; hydroxyapatite; composite materials; dental pulp stem cells; dental regeneration

## ABBREVIATIONS

CM-CS, carboxymethyl chitosan; HA, hydroxyapatite; CaP, Calcium Phosphate; BDGE, 1,4-butanediol diglycidyl ether; ESEM, environmental scanning electron microscope; XRD, X-ray diffraction; hDPSCs, human dental pulp stem cells; ATR-FTIR, attenuated total reflectance fourier transform infrared spectroscopy; BSA, bovine serum albumin

## INTRODUCTION

Dental caries are the most prevalent yet preventable disease in both children and adults [1]. Current treatments center around the restoration of tooth function based on dental fillings that fill the defect and prevent further decomposition of the tooth matrix while returning the ability to comfortably chew. Dental caries come in a variety of severities, from insipient (less than halfway through the enamel) to severe (more than halfway to the pulp) [2]. Those with severe caries face the possibility of losing the tooth all together.

From the most recent sources, 90.9% of US adults aged 20–64 have at least one dental cavity, and 27% go untreated [3]. The most prevalent restorative methods for cavity treatment are amalgam and resin fillings. These fillings have an estimated lifetime of 10–15 years, and 7–10 years respectively, as defined by the time in which it either becomes degraded and is no longer performing its function, or that a secondary cavity has formed within the boundary of the filling and that it must be removed, cleaned, and replaced with a new one [4]. Most people with some level of severe tooth decay will have to face pulp capping or a root canal. If a cavity becomes so severe that it threatens to infect the dental pulp, it may be necessary to apply a pulp capping agent to save the tooth. Pulp capping is the method of activating a regenerative response by the dental pulp tissue to reform or protect the remaining tissue from becoming infected [5–8]. Many different materials have been used as pulp capping agents with various levels of success in forming a dentin bridge that seals the pulp. The gold standard for pulp capping is calcium hydroxide, which creates a necrotic layer of pulp that seals the vital tissue and stimulates the formation of a dentin bridge [9]. The disadvantage of calcium hydroxide is related to the dissolution away from the repair site and into the pulpal chamber which can cause extensive mineral formation [10,11].

Pulp capping agents must exhibit properties such as retaining pulp vitality, stimulating reparative dentin, adhering to both the dentin and filling material, and remaining mechanically stable during filling placement [11]. Many types of minerals, biopolymers, and cements have been devised to exhibit these properties, but none have been able to fill all these roles and facilitate the native regeneration of dentin tissue [12,13].

This work presents a new pulp capping agent that can be used to meet the necessary properties with added functionality. Ideally such a material must be injectable, fast setting, mechanically stable, biocompatible and odontogenic. Injectability and relatively fast setting times are required for practical use in the clinical setting. Mechanical stability protects the vulnerable pulp and provides a stable surface for subsequent layers of restorative filling. Biocompatibility and odontogenicity are important to maintain pulp viability, increase cellular proliferation into the scaffold interior, and to promote the differentiation of dental pulp stem cells into odontoblastic cells for remodeling the dentin tissue.

Here we describe a composite material containing a polymer phase of carboxymethyl-chitosan (CM-CS), a composite phase of hydroxyapatite (HA) whiskers, and a crosslinking agent 1,4-butanediol diglycidyl ether (BDGE) (Figure 1). The compressive modulus of these materials is demonstrated to be as high as 600 kPa, which is greater than the typical pulp capping agent, calcium hydroxide. These composites are injectable and moldable within the gelation time of 20 min. These materials support the growth of cells for up to 3 weeks and show odontogenic markers such as RUNX2 and osteocalcin. Thus, these materials show promise as a new generation of regenerative pulp capping materials.
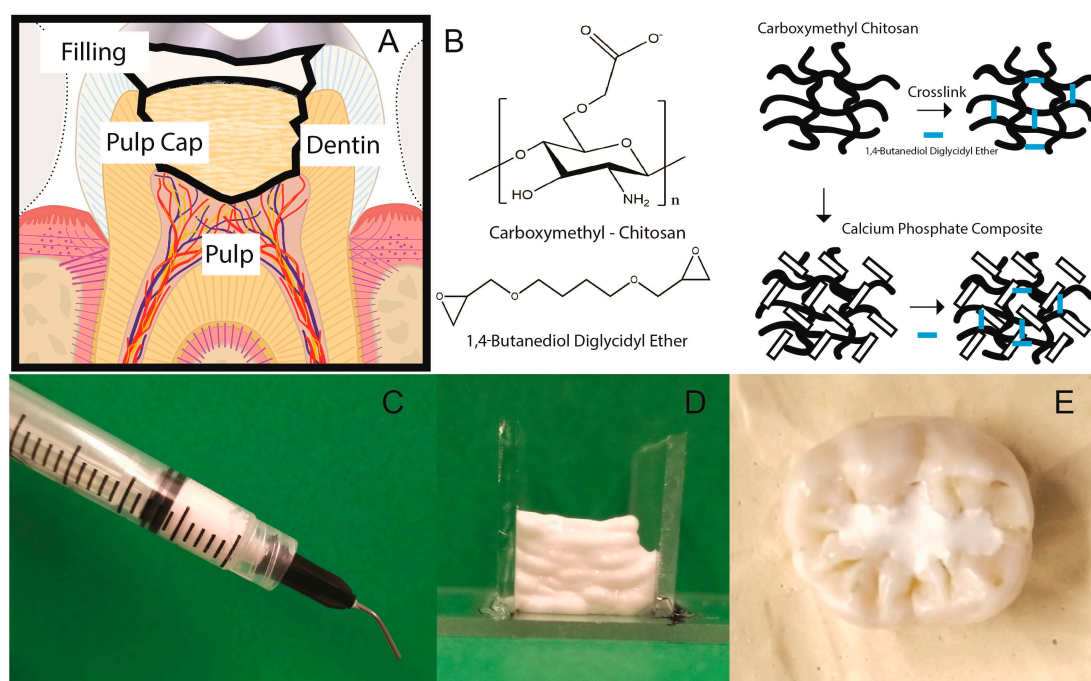


**Figure 1.** (**A**) Diagram of a tooth illustrating the locations of a filling, pulp capping agent, dentin tissue, and dental pulp. (**B**) Diagram illustrating the carboxymethyl-chitosan polymer, and crosslinking agent and composite crosslinking. (**C**) Syringe filled with injectable pulp capping agent. (**D**) Applied pulp capping agent with self-supporting structure. (**E**) Pulp capping agent applied to drilled and prepared tooth.

## MATERIALS AND METHODS

### Materials

Chitosan (medium molecular weight, 190–310 kDa), chloroacetic acid, calcium nitrate, ammonium phosphate, acetamide, 1,4-butanediol diglycidyl ether and TRI Reagent were all purchased from Millipore Sigma (St. Louis, MO, USA) at reagent grade (>99%) and used as is. Nitric acid (6 M) was purchased from Carolina Biological Supply Company (Burlington, NC, USA). Human dental pulp stem cells (hDPSCs) were obtained from Lonza (Walkersville, MD, USA). 4,6-Diamidino-2-phenylindole, dihydrochloride (DAPI), Osteocalcin Monoclonal Antibody (OCG4) and Goat anti-Mouse IgG (H + L) highly cross-absorbed secondary antibody,

AlexaFluor Plus 647 were all purchased from ThermoFisher (Waltham, MA, USA).

**Synthesis of Carboxymethyl Chitosan**

Carboxymethyl chitosan (CM-CS) was synthesized using a procedure outlined by Chen and Park [14]. Briefly, medium molecular weight chitosan was dissolved in 80% isopropyl alcohol at a concentration of 0.135 g/mL and maintained at 50 °C for 1 h until completely wetted and well mixed. Monochloroacetic acid was dissolved in pure isopropyl alcohol at a concentration of 0.75 g/mL, added dropwise to the chitosan solution, and this mixture reacted for 4 h at 50 °C. The reaction was quenched by 200 mL of absolute ethanol. The solids were then filtered through a 22-µm filter and rinsed several times, gradually increasing from 70% to absolute ethanol and dried under vacuum at room temperature. The CM-CS was then dissolved in Millipore water at 1% *w*/*v*, filtered through a 22-µm filter, frozen, and lyophilized until further use.

**Synthesis of Hydroxyapatite Whiskers**

Hydroxyapatite (HA) whiskers were synthesized using a method previously outlined by Zhang *et al.* [15,16]. Briefly, a solution of 50 mM nitric acid was used to dissolve 42 mM calcium nitrate, 25 mM ammonium phosphate, and 1 M acetamide. The solution was adjusted to pH 3.0 using either 1 M ammonium hydroxide or 1 M nitric acid. This solution was placed into a 500 mL hydrothermal synthesis reactor and heated to 180 °C for 12 h. The reactor was cooled slowly to room temperature and then filtered using a 22-µm filter. The whiskers were then rinsed three times with Millipore water and dried at 80 °C for 3 h.

**X-ray Diffraction (XRD) Analysis**

X-ray diffraction patterns of the HA whiskers were obtained using powder diffraction on a Siemens D500 (KS Analytical Systems, Aubrey, TX, USA) operating in the symmetric Bragg-Brentano mode, with a Cu X-ray tube and a graphite monochromator.

**Composite Hydrogel Fabrication**

Composite hydrogels were made with varied amount of HA whiskers (0 wt %, 30 wt %, or 40 wt %). A 10% (*w*/*v*) solution of CM-CS was made using phosphate buffered saline (PBS) at pH 7.4. Then 1 mL CM-CS solution was drawn into a 3 mL syringe. For the 0 wt % HA hydrogels, 50 µL of 1,4-butanediol diglycidyl ether (BDGE) was placed in another 3 mL syringe. The syringes were connected, and the two solutions were mixed vigorously for 15 s before being injected into a 12 well plate as a circular mold. For the 30 wt % and 40 wt % HA hydrogels, 428 mg and 666 mg of the HA whiskers, respectively, were measured into a 3 mL syringe. This syringe was then connected to the syringe containing the CM-CS

solution to mix the CM-CS and HA whiskers together until visually homogeneous. These syringes were then centrifuged at 1000× g for 5 min to remove any bubbles that may have been formed during mixing. Next, 50 µL of BDGE was mixed with the composite mixture for 15 s before being injected into the mold. All scaffolds were allowed at least 4 h at 37 °C to completely crosslink. The scaffolds that were used for cell seeding were punched using a 5 mm biopsy punch, sterilized in 70% ethanol and placed under UV light for 1 h, and rinsed 3 times with sterile PBS.

### Environmental Scanning Electron Microscopy (ESEM)

The surface microarchitecture of the composite hydrogels was examined using a FEI Quanta 600i Environmental Scanning Electron Microscope (Hillsboro, OR, USA). Scaffolds were air dried and sputter coated with gold. Images were taken from 10 mm using 20 kV accelerating voltage.

### Infrared (IR) Spectrum Analysis

IR spectra were obtained using a Nicolet™ iN™ 10 MX Infrared Imaging Microscope with the micro-attenuated total reflectance (ATR) attachment. Air dried composite hydrogels were placed on microscope slides and the micro-ATR attachment was lowered to touch the flattest part of the gel with 2 psi.

### Rheological and Dynamic Mechanical Analysis

Gelation experiments were performed on an AR-G2 rheometer (TA Instruments, New Castle, DE, USA) using a 20 mm cross-hatched Peltier Plate geometry and a solvent trap. Composite hydrogels used for rheology were produced using the same method as described above, reducing the total volume to half the original volume. After mixing the CM-CS solution, HA whiskers, and BDGE, the composite was placed in the center of the rheometer plate and the geometry was lowered to a gap height of 1500 µm. The solvent trap was applied and filled with distilled water to prevent evaporation from the hydrogel. Time sweeps were performed at 37 °C using a frequency of 1 Hz at 5% strain for up to 2 h to determine the total time required for the hydrogel to gel. The gelation time was determined at the time when the storage and loss modulus cross. Compressive modulus was measured using dynamic mechanical analysis on an ARES-G2 rheometer (TA Instruments, New Castle, DE, USA). Hydrogel composites were fabricated as described above. Composites that were cured overnight were placed between two 20 mm parallel plates. A strain sweep was performed from 0.1% to 10% at a frequency of 1 Hz. Moduli reported are taken at 1% strain for comparison.

**Swelling and Degradation**

The swelling and degradation properties of the composite hydrogels were determined by placing each gel in 5 mL of simulated saliva solution [17] and incubating at 37 °C. At intervals of 12 h, 1, 3, and 7 days the gels were weighed after blotting the surface dry to obtain the mass of the swollen gels. Each of these gels were then frozen, lyophilized, and weighed to determine the degradation. The swelling percent of the hydrogels was calculated using Equation 1 defined below:

$$\% \text{ Swelling} = \frac{\left(\text{Mass of Swollen Gel} - \text{Mass of Dry Gel}\right)}{\text{Mass of Dry Gel}} - \frac{\text{Initial Mass of Water}}{\text{Initial Mass of Dry Gel}} \quad (1)$$

The swelling percent is calculated for each time point and the initial swelling percent is subtracted to account for the different initial amounts of water within each gel variant.

The percent swelling is determined at every time point. The initial % swelling is subtracted to account for the initial amount of water contained in each gel. The dried weight of each gel was used to calculate the degradation percent for each gel type, defined using Equation 2 below:

$$\% \text{ Degradation} = \frac{\text{Initial Dry Mass} - \text{Dry Mass}}{\text{Initial Dry Mass}} \quad (2)$$

The dry masses of the composite hydrogels were used to determine the extent to which the polymer network or calcium phosphate composites break down or leach out over time, and to negate swelling effects.

**Human Dental Pulp Stem Cell (hDPSC) Seeding and Culture**

hDPSCs were cultured using alpha-MEM without nucleosides + 16.5% FBS + 2 mM L-glutamine + penicillin/streptomycin (100 units/mL and 100 µg/mL, respectively). Cells were maintained in a humidified incubator at 37 °C and 5% $CO_2$. All cells were used at passage 4. Sterile composite hydrogels were placed into sterile non-tissue culture 96-well plates and incubated in 100 µL alpha-MEM for 1 h prior to cell seeding. The culture media was aspirated from the hydrogels and 20 µL containing 10,000 hDPSCs was placed on top of each gel. All gels were then incubated for 3 h and then 100 µL of culture media was added. The media was changed every 3 days for the duration of the experiment.

**hDPSC Proliferation**

A DNA assay was performed on days 3, 7, 14, and 21 to determine the relative number of cells on each composite hydrogel over time. Each scaffold was placed into an RNase/DNase free microcentrifuge tube with 500 µL of papain buffer (25 µg/mL papain extract from papaya, 2 mM *N*-acetyl cysteine, 2 mM EDTA, and 50 mM sodium phosphate, adjusted to pH 6.5 using 1 M HCl) and sonicated at 50 Hz for 15 s. These scaffolds

were then incubated at 65 °C for 3 h. After incubation, each tube was centrifuged at 10,000× g for 10 min to pellet any remaining insoluble fragments. Using a Quant-iT PicoGreen dsDNA assay kit (Invitrogen, Carlsbad, CA, USA) the DNA concentration was determined from the supernatant as per the manufacturer's protocol on a Synergy H1 plate reader (BioTek, Winooski, VT, USA). The DNA concentration was determined by comparison with a standard curve created from calf thymus DNA.

## Immunostaining and Confocal Imaging

Fluorescent stains were used to visualize the hDPSCs on the CM-CS-HA composite hydrogels over a 3-week period. The hDPSC-laden scaffolds were fixed using 10% Neutral Buffered Formalin overnight at 4 °C. Scaffolds were rinsed three times with PBS. Each scaffold was permeabilized using 0.1% Triton X-100 for 15 min at room temperature, then rinsed three times with PBS for 5 min each. Each hydrogel was blocked using 5% Goat serum for 1 h and rinsed three times. Hydrogels were soaked in 10 μg/mL primary antibody (Mouse Anti-Human Osteocalcin, Invitrogen) overnight at 4 °C and rinsed three times, then soaked in the secondary antibody at 10 μg/mL (Goat Anti-Mouse IGG with Alexa Fluor Plus 647, Invitrogen) for 2 h, then rinsed three times. Finally, hydrogels were placed in 1 μg/mL 4,6-diamidino-2-phenylindole (DAPI) solution. The samples were then imaged on a Nikon eclipse Ti microscope running NIS elements AR software.

## RNA Isolation and qPCR

RNA was isolated from samples at 7, 14, and 21 days. Cells were cultured on hydrogels placed in 24 well plates with 50,000 cells seeded initially. At each timepoint, total RNA was isolated using TRI Reagent as per manufacturer's instructions. RNA quantity and purity was measured using a Synergy H1 plate reader (BioTek, Winooski, VT, USA) with a Take3 microplate. RNA was reverse transcribed using a High-Capacity cDNA Reverse Transcription Kit (Applied Biosystems, Foster City, CA, USA). Real-time quantitative PCR (RT-qPCR) was used to measure the relative expression of osteogenic transcription factor RUNX2. Primers were designed using Primer Blast (NCBI, Bethesda, MD, USA) for all variants of human RUNX2 and human GAPDH. For RUNX2, left primer was 5'–GAC GAG GCA AGA GTT TCA CC–3' and right primer 5'–AGC TTC TGT CTG TGC CTT CT–3', GAPDH left primer 5'–TGT CAA GCT CAT TTC CTG GTA TG–3' and right primer 5'–GTG GTC AGG GGT CT TAC TC–3'. RT-qPCR was performed on a Roche LightCycler 480 instrument (Roche, Basel, Switzerland) using PowerUp SYBR Green Master Mix (Applied Biosystems).

### Protein Loading and Release

HA whiskers were loaded with bovine serum albumin (BSA) by being soaking 1 g whiskers in a solution of 10 mg/mL BSA. The BSA was loaded onto the Calcium Phosphate (CaP) nanoparticles for 48 h, before being centrifuged at 10,000× g for 5 min. The supernatant was collected to determine the amount of BSA loaded.

The loaded whiskers were rinsed to remove any loosely bound BSA and then lyophilized to produce a dry powder. This powder was then used to make composite hydrogels the same as previously described. Hydrogels were placed into microcentrifuge tubes and 1 mL of PBS was used as a release media. The samples were placed on a rotator in a 37 °C incubator during the release. At each time point, each microcentrifuge tube was centrifuged at 10,000× g for 5 min and the supernatant was collected in a separate tube and replaced with 1 mL PBS. A microBCA assay was used to compare and measure the amount of BSA present in both the loading solutions and release solutions.

### Statistical Analysis

All experimental data ($n$ = 4) are expressed as mean ± standard deviation. All data sets were compared using a 2-way ANOVA with post hoc Tukey HSD test for individual comparisons. Differences between experimental groups were considered significantly different when $p < 0.05$.

### RESULTS

### Material Characterization

Hydroxyapatite whiskers were synthesized as the composite filler for these materials, due to their similarity to native calcium phosphate mineral and their desirable properties as a filler. The HA whiskers were characterized by XRD. The XRD patterns, shown in Figure 2, exhibit the same characteristic HA peaks as those presented by Zhang *et al.*, with the peaks labeled (100), (200) (210), (211), and (300). The peak at (300) is the strongest XRD peak where HA is typically at (211), this shows a bias for the (300) plane in the presence of these whiskers [15].

For the polymer phase for these materials, carboxymethyl chitosan was fabricated. This material was selected as it is a water-soluble polymer that is still able to crosslink via epoxides to form a self-setting material. The successful functionalization of chitosan into carboxymethyl chitosan is demonstrated by the FTIR spectra displayed in Figure 3. The characteristic peak of the primary amine stretch is located at 1312 cm$^{-1}$, while the characteristic stretch of the COO$^-$ group at 1600 cm$^{-1}$ identifies the carboxyl group. The carboxyl group is shifted from the typical 1741 cm$^{-1}$ because it is in the form of a carboxylate salt containing Na$^+$. The sharp peak on Figure 3A at 1600 cm$^{-1}$ can also be an overlap of the primary amine (1592 cm$^{-1}$). The FTIR spectra of the hydrogels and the hydroxyapatite whiskers were then compared to the composite hydrogels

(Figure 3B). These spectra confirm the composite nature of these HA-laden hydrogels, with the carboxylate group present in the gels and the inorganic phosphate ($PO_4^{3-}$) at 1034 cm$^{-1}$ [15].
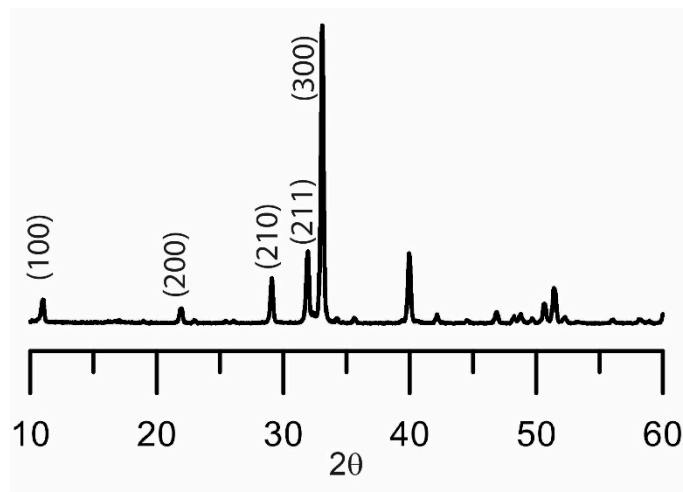


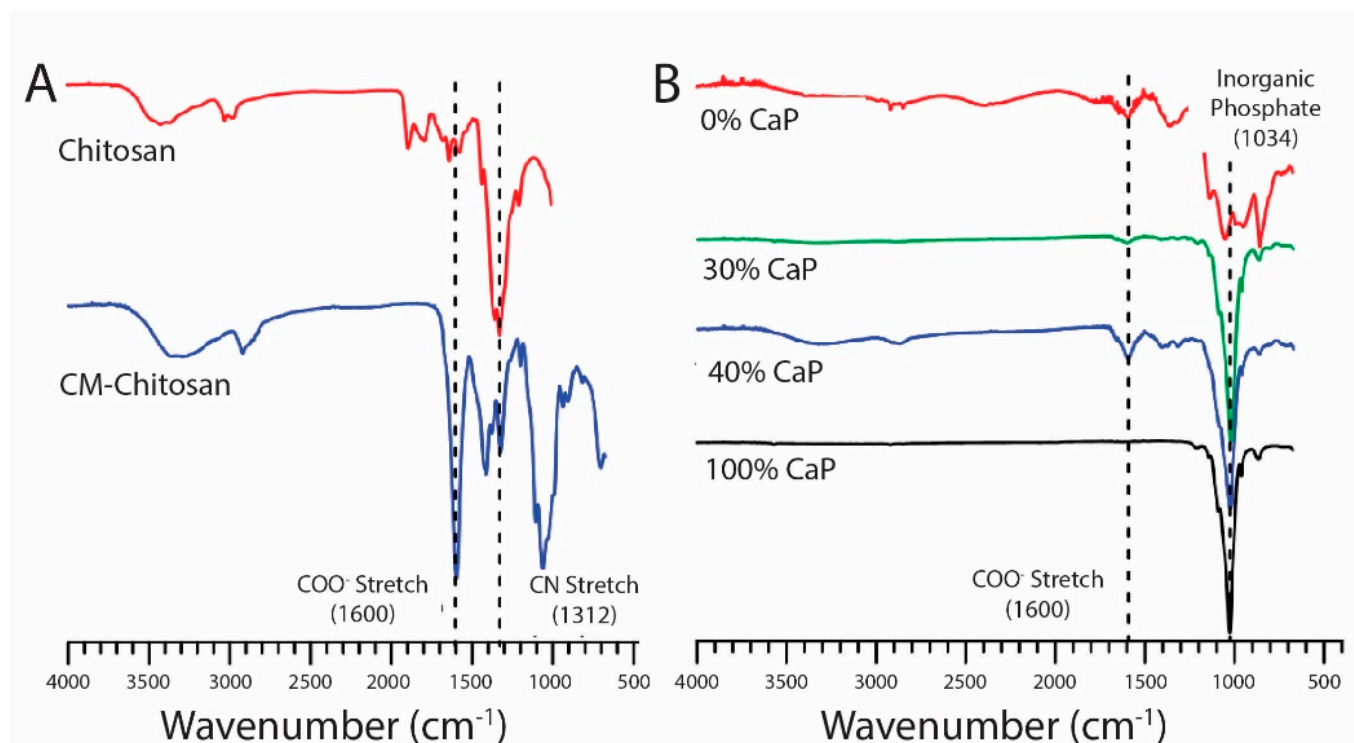**Figure 2.** X-ray diffraction pattern of hydroxyapatite whiskers.



**Figure 3.** (**A**) FT-IR spectra of chitosan and carboxymethyl-chitosan. (**B**) FTIR spectra of the formed composite hydrogels with 0, 30, or 40 wt % hydroxyapatite whiskers, and pure hydroxyapatite whiskers.

The surface characteristics of the composite materials were examined via SEM. Scanning electron photomicrographs show the shape and size of the hydroxyapatite whiskers alone (Figure 4A). Whiskers are shown to have a high aspect ratio and to be relatively consistent. HA whiskers fabricated using this methodology were measured previously by us to be 55 ± 30 μm long by 5 ± 2 μm in diameter [16]. SEM images of the dried

composite hydrogels for the 30 wt % and 40 wt % composites show the surface roughness and porosity (Figure 4B,C).
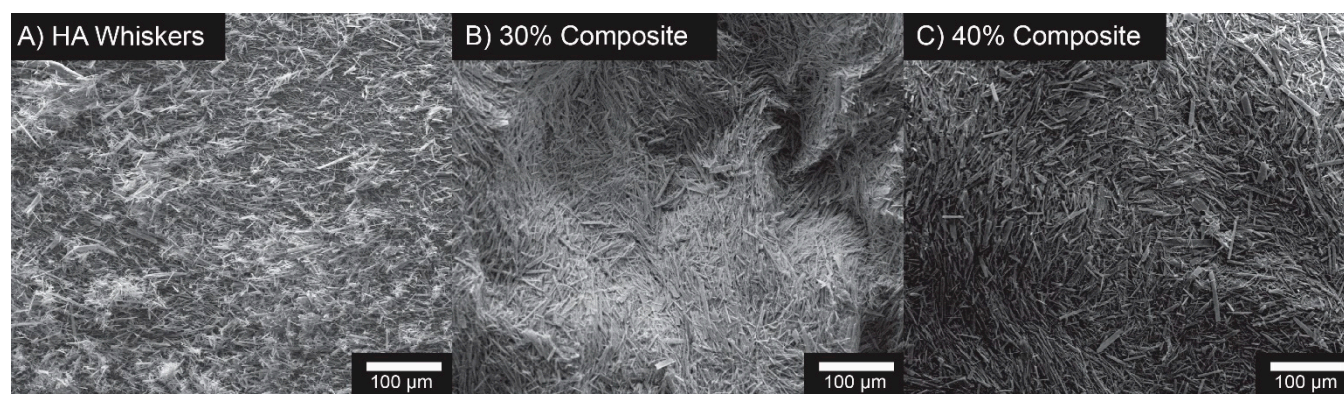


**Figure 4.** Scanning electron photomicrographs of (**A**) hydroxyapatite whiskers, (**B**) the surface of the 30 wt % and (**C**) the surface of the 40 wt % composites. Scale bars are 100 μm.

**Table 1.** Gelation times determined by time sweep rheology. ($n$ = 3) This data set was compared using a 1-way ANOVA with post hoc Tukey HSD test for individual comparisons, and the following $p$-values were found: $p$ = 0.038 between 0 and 30 wt %, $p$ = 0.702 between 0 and 40 wt %, and $p$ = 0.015 between 30 and 40 wt %.

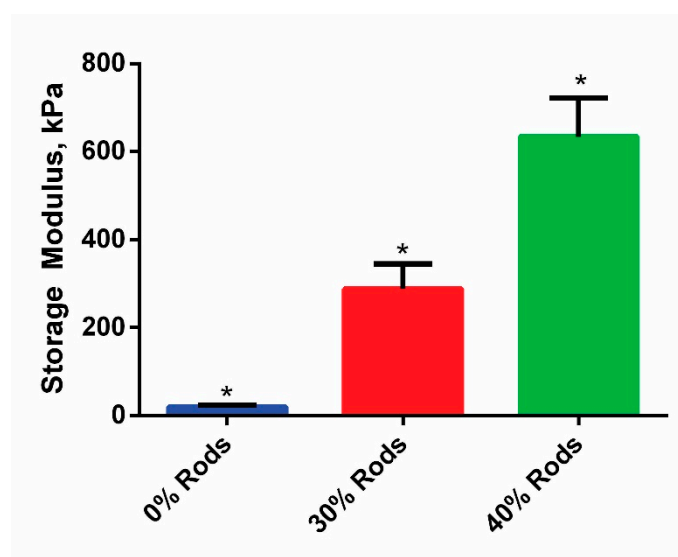| Composite wt % | Gelation Time, min |
|---|---|
| 0 wt % | 17.29 ± 0.05 |
| 30 wt % | 15.83 ± 0.4 |
| 40 wt % | 17.66 ± 0.85 |



**Figure 5.** Storage modulus of the composite materials measured by dynamic mechanical analysis. ($n$ = 4, * $p$ = 0.0039 for 30 wt %, and $p$ = 0.0001 for 40 wt % compared to 0 wt %) This data set was compared using a 1-way ANOVA with post hoc Tukey HSD test for individual comparisons.

The initial viscosity of each of the gels was 30,000 cP which gradually increased during crosslinking. The gelation times for each type of composite hydrogel was measured using time sweep rheology. All types

gelled around 16–17 min (Table 1). To quantify the mechanical properties of these materials, the compressive modulus was measured by dynamic mechanical analysis. It was found that the storage modulus increased as the incorporation of HA whiskers increased (Figure 5). The modulus of the CMCS hydrogel alone is 19 kPa. As the composition of the whiskers is increased to 30 wt % and then 40 wt %, the storage modulus increased to 287 kPa and 633 kPa, respectively. Thus, greater amounts of HA whiskers contribute to higher mechanical properties of the materials. Above 40 wt % loading the composite hydrogels become so saturated with solid that it is too difficult to create a homogenous mixture, and the polymer network is too sparse to crosslink. Thus, 40 wt % was the maximum amount of filler examined in these studies.
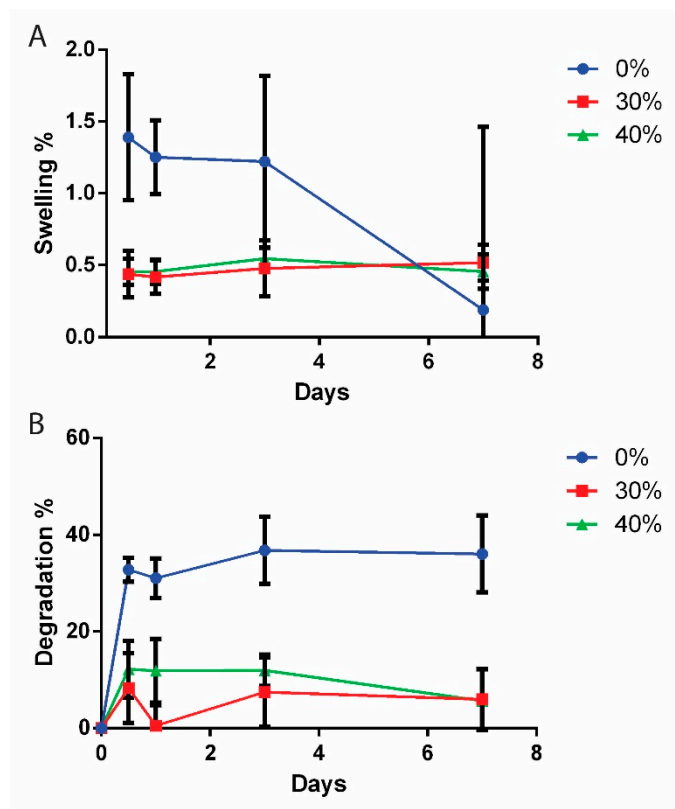


**Figure 6.** (**A**) Swelling and (**B**) degradation percent for 0 wt %, 30 wt %, and 40 wt % composite hydrogels ($n$ = 4).

The swelling and degradation rates of these composite materials over time was measured to further characterize them. The swelling percent quantifies the amount of water these gels will uptake after being fabricated. It was found that most of the swelling in these materials occurs within the first 12 h after being placed in swelling medium (Figure 6A). The 0 wt % hydrogels have the highest amount of swelling with a 1.4% average increase in water, while the 30 wt % and 40 wt % composites increase only by 0.5%.

Additionally, the rate of degradation of the materials over time was quantified. The 0 wt % hydrogels demonstrate the greatest amount of

early degradation (Figure 6B) at almost a 40% decrease in dry weight in less than a day, whereas the composite materials show less degradation (less than 10%) over time.

### Human Dental Pulp Stem Cell Interaction with the Composite Hydrogels

Human dental pulp stem cells were seeded on the composite materials to determine their ability to proliferate and differentiate. DNA was quantified to determine the relative growth of cells that were seeded on the top surface of each type of composite hydrogel (Figure 7). The 0 wt % hydrogels had the lowest amount of cellular proliferation and decreased below the limit of detection during the 3rd week. The 30 wt % and 40 wt % composite hydrogels had the same amount of proliferation as each other over 3 weeks of culture, with no significant difference between these two composites at each timepoint. The highest amount of DNA was measured at the beginning of the experiment.
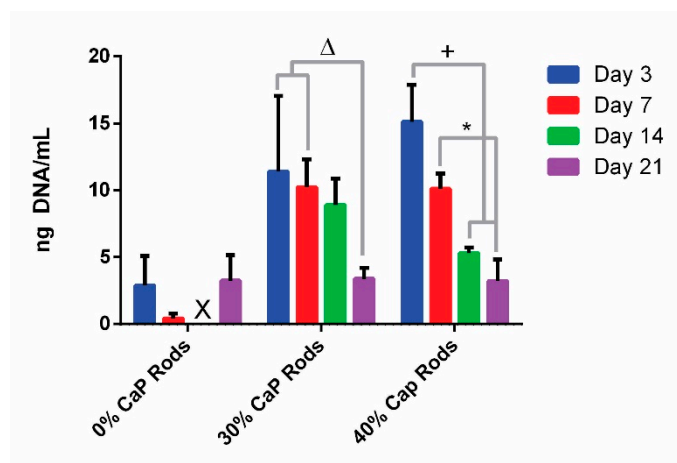


**Figure 7.** DNA quantification from human dental pulp stem cells grown on dental composite materials. ($n$ = 4, Δ $p$ = 0.0.0014 and 0.0334 for day 3 and 7 (respectively) compared to day 21; + $p$ = 0.0001 for both day 14 and 21 compared to day 3, and * $p$ = 0.006 for day 7 compared to day 21). This data set was compared using a 2-way ANOVA with post hoc Tukey HSD test for individual comparisons.

The differentiation of the hDPSCs over time was quantified based on measurement of mRNA expression of RUNX2, an important osteogenic transcription factor, and osteocalcin immunostaining. Quantitative PCR was used to measure the relative amount of RUNX2 expression in hDPSCs cultured on these materials for 2 and 3 weeks (Figure 8). This data is analyzed using the $\Delta\Delta C_t$ method and displayed here as a fold change of expression compared to the 0 wt % materials. At week 2, the expression of RUNX2 is significantly higher for both 30 wt % and 40 wt % composite hydrogels compared with the 0 wt % hydrogels, but not significantly different from each other. By 3 weeks of culture, the expression of RUNX2 had decreased and was statistically the same for all three materials.
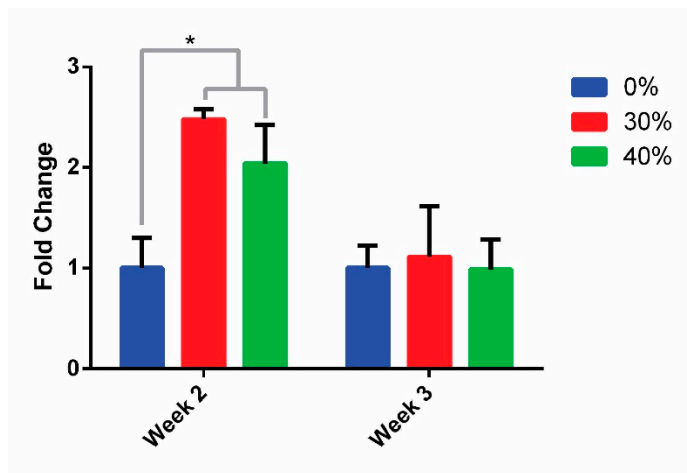
**Figure 8.** qPCR analysis of RUNX2 expression for 0 wt %, 30 wt %, and 40 wt % dental composite materials, using 0 wt % materials as the comparison group. ($n$ = 4, * $p$ = 0.0001 for 30 wt % and $p$ = 0.0016 for 40 wt % compared to 0 wt %) This data set was compared using a 2-way ANOVA with post hoc Tukey HSD test for individual comparisons.
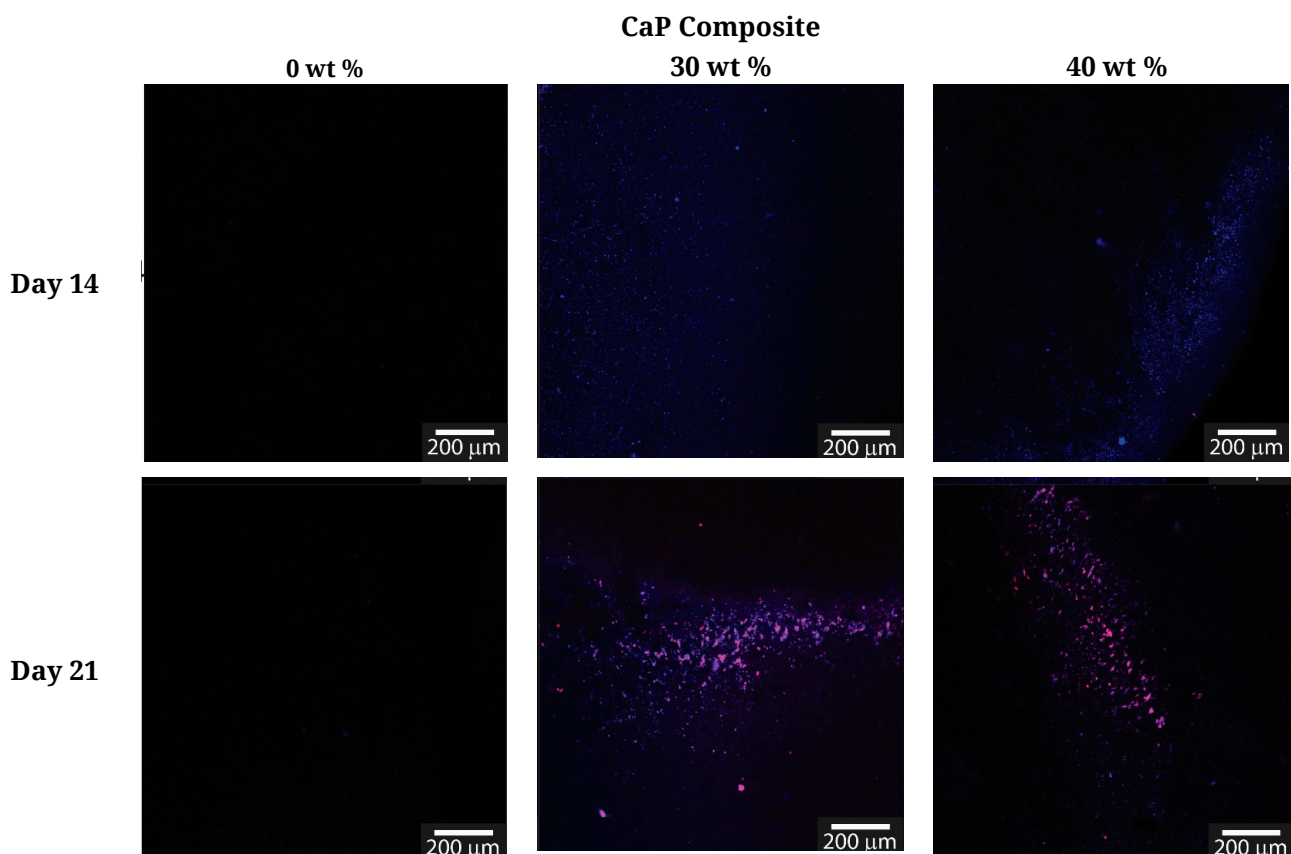


**Figure 9.** Confocal micrographs of hDPSCs grown on dental composite materials for 14 and 21 days. Cell nuclei are stained with DAPI (blue) and osteocalcin is stained with Alexa Fluor Plus 647 (pink). Scale bars are 200 µm.

To visualize the cells on the materials, and to visualize their expression of osteocalcin, a marker for odontogenic differentiation, fluorescent confocal micrographs were taken of the cells seeded on the surface of each composite hydrogel after 14 and 21 days of culture. The

nuclei were stained blue with DAPI and osteocalcin-antibodies were used to stained osteocalcin pink (Figure 9). The 0 wt % hydrogels showed little proliferation and cells were difficult to locate at both timepoints. On the materials containing 30 wt % and 40 wt % HA whiskers, cells are visible across the materials at 14 days, but no osteocalcin is visible on either scaffold type. By 21 days, osteocalcin is visible around each cell on these materials, indicating that the hDPSCs are differentiating down the odontogenic lineage.

**Sustained Protein Release from the Composite Hydrogel Materials**

These composite materials were also evaluated as a possible device for controlled release of proteins. Bovine serum albumin was used as a model protein to determine the quantity of protein that could be loaded and the rate of release over time. The amount of BSA that could be loaded in the materials was directly related to the quantity of HA whiskers that were loaded in the hydrogels (Figure 10A), with twice as much BSA loaded in the 40 wt % composite gels compared to the 20 wt %. 20 wt % was chosen to gain a higher divergence of the release profiles to elucidate the effects of HA whiskers on protein release. Next, the release of BSA over time was measured, and it was found that the release was sustained for at least 15 days (Figure 10B).
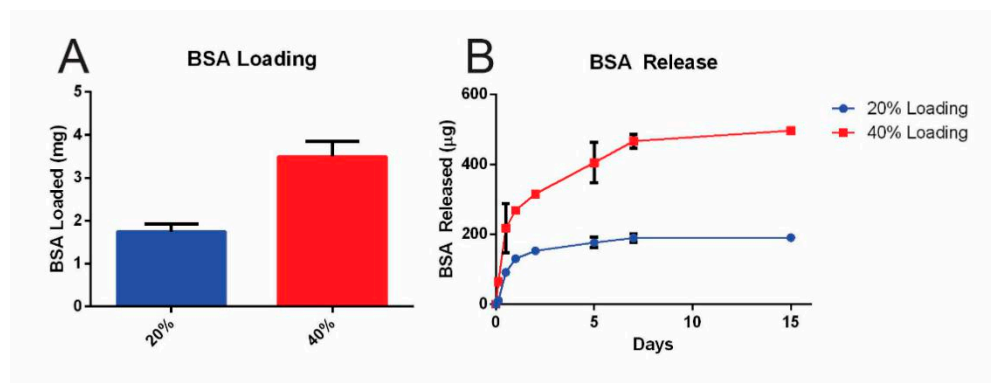


**Figure 10.** (**A**) Bovine serum albumin loading into the composite gels and (**B**) release of BSA from composite gels over 2 weeks (*n* = 4).

**DISCUSSION**

The mineral phase of these composite hydrogels was chosen to be HA whiskers as they would provide mechanical strength, bioactivity, and a unique morphology to a regenerative filling [15,18]. HA is similar to the calcium phosphate that is found in native mineralized tissues, and has been shown to promote osteogenic differentiation [19–21]. These whiskers can be readily manufactured and have been previously characterized and used by other groups as well.

Chitosan is a natural polysaccharide derived from chitin that is found in the shells of crustaceans and processed to provide a polymer made up of D-glucosamine. The main functional group of D-glucosamine is the

primary amine. For this composite material, we desired to use the primary amines to crosslink the polymer with diglycidyl ethers. However, if the chitosan were solubilized in a typical acidic environment, these primary amines would be protonated, which can prevent their reaction with epoxide groups. Thus, to improve the solubility of chitosan while also protecting the amine groups, we functionalized the available hydroxyl groups with carboxymethyl groups. This method yields a chitosan with a hydrophilic carboxyl group at pH 7.4 while also keeping the primary amines deprotonated so that they are still capable of reacting with the crosslinking agent.

When combined into a composite material, the organization and alignment of the whiskers along the surface of the hydrogels appears to be random. The 40 wt % composites have a greater mineral to polymer ratio, which can be visualized in their surface topology compared to the 30 wt % composites. Surface topology with nanostructured roughness (<100 nm) has been shown by others to increase proliferation of cells, while greater roughness can hinder cell proliferation but with the benefit of increased differentiation potential [22]. These composite materials do not appear to contain large pores that penetrate the interior of the material, which may limit cell migration into the interior of the material initially until biodegradation occurs at later times.

The mechanical properties of composites are affected by many factors, including the shape, size, and volume percentage of the filler, the properties of the polymer matrix, and the interaction between these two phases [23]. To use these materials as a regenerative material, it is important to balance high strength materials with water content and porosity. These composite materials must have mechanical strength high enough to withstand the forces associated with their application in the dental cavity. However, also to consider is the tradeoff that with greater mechanical properties is the reduction of relative water content and porosity that are important to support cell growth and proliferation. These composite materials do not have mechanical strength equivalent to typical mineral trioxide and composite resin materials, but they are strong, and they do have 60 to 70% water content which provides an environment to sustain cell growth.

It is important to minimize the amount of swelling that fillings exhibit so that they do not swell out of the filling space that they were applied to or delaminate from the dentin surface. Here we show that the equilibrium swelling of these composite gels was very close to their initial fabrication amounts which would be beneficial when applied to the hydrated oral environment. The equilibrium swelling of the composite materials is equivalent or lower than typical dental composite resins [18]. It is also important to minimize the initial amount of degradation these fillings undergo so that they do not disintegrate shortly after they are applied to dental caries. These materials exhibit low degradation over at least 7 days. The swelling and degradation both reach equilibrium

quickly and little change occurs over the next 7 days. The initial rapid degradation of 0 wt % hydrogels is likely to be due to a removal of any unreacted or loosely bound CM-CS as it does not continue to degrade after equilibrium is reached. The composite hydrogels degrade less because the weight of the HA whiskers is greater than the amount of CM-CS. The low swelling and degradation of these composites show promise for increasing the lifetime of the fillings.

The material properties of the composites are very promising as shown, but also important is their ability to interact with regenerative cells. Thus, hDPSCs were seeded on the materials, and both their proliferation and their differentiation measured at various times. In terms of proliferation, the lack of measurable DNA on the 0 wt % hydrogels demonstrate that the stem cells cannot adhere to or proliferate on the polymer alone over time. This is because the chitosan itself does not have binding sites for cells to attach. The addition of HA whiskers provides binding sites for cells to attach to, and thus the materials that contain HA whiskers supported cell adhesion. For both the 30 wt % and 40 wt % hydrogels, the amount of DNA decreased over time. This decline in proliferation is because the cells reached confluency early in the experiment due to minimal material porosity that would allow cells to migrate into the scaffold [22]. In terms of differentiation, the gene expression of RUNX2, a major odontogenic transcription factor, of hDPSCs on these materials was quantified by qPCR [24,25]. Scaffolds that contained HA whiskers had an elevated amount of RUNX2 expression, and therefore a greater amount of differentiation, due to the interaction of the cells with HA. Additionally, confocal images show the appearance of osteocalcin at 21 days of culture. Osteocalcin is a late stage osteogenic marker which indicates that the cells have progressed to odontoblastic cells. The presence of osteocalcin is only seen on scaffolds that contained HA whiskers, further illustrating the importance of HA in the differentiation process. It is important to note that these cells were not cultured in differentiation media for any of these experiments, so their response is due solely to the presence of HA.

Finally, the ability for these materials to deliver proteins in a sustained manner over time was investigated, as this could be impactful in the future for encouraging tissue regeneration by the inclusion of chemokines or cytokines. Here a model protein, BSA, was used as a proof of concept. BSA has been shown to readily adsorb onto the surface of many types of HA [26,27]. The adsorption of BSA onto HA whiskers is hypothesized to protect the BSA from being crosslinked into the polymer network. Although higher released amounts were obtained with higher HA whisker weight percent, the rate of release over time was not significantly affected. This protein adsorption mechanism may be used as a strategy for other biologically active proteins. The release of chemokines and growth factors is a well-known strategy for improving the biological interaction between tissue scaffolds and native cells. Thus,

the ability for these materials to sustain some level of protein delivery shows promise for future integration of factors that may be used to stimulate the migration of cells, particularly hDPSCs, further into the scaffold.

## CONCLUSIONS

These CaP-CMCS composite materials show promise as a potential regenerative pulp capping material. These composites meet important objectives for an effective pulp capping agent including fast gelation, improved mechanical properties, biological compatibility, and odontogenic potential. Future studies will investigate the use of different calcium phosphate particles as the filler material, and the incorporation of chemokines and cytokines for improved migration of pulp cells into the filling materials.

## AUTHOR CONTRIBUTIONS

MJO and RRM performed the experiments, and both MJO and MDK contributed to designing the studies, analyzing the data, and writing the paper.

## CONFLICTS OF INTEREST

The authors declare that they have no conflicts of interest.

## FUNDING

## REFERENCES

1. Trends in oral health status: United States, 1988–1994 and 1999–2004. Dye BA, Tan S, Smith V, Lewis BG, Barker LK, Thornton-Evans G, et al., editors. Hyattsville, (MD, US): Department of Health and Human Services, Centers for Disease Control and Prevention, National Center for Health Statistics; 2007.

2. Must-know classifications of dental caries for the national dental hygiene boards. Available from: https://www.dentistryiq.com/articles/2016/03/must-know-classifications-of-dental-caries-for-the-national-dental-hygiene-boards.html. Accessed 2019 Jan 3.

3. Dye BA, Iafolla TJ. Dental Caries and Tooth Loss in Adults in the United States, 2011–2012. NCHS Data Brief. 2015 May;197:197.

4. The facts on fillings: Amalgam *vs*. resin composite. Available from: https://www.deltadentalins.com/oral_health/amalgam.html. Accessed 2019 Jan 3.

5. Komabayashi T, Zhu Q, Eberhart R, Imai Y. Current status of direct pulp-capping materials for permanent teeth. Dent Mater J. 2016;35:1-12. doi: 10.4012/dmj.2015-013

6. Schwendicke F, Stolpe M. Direct Pulp Capping after a Carious Exposure Versus Root Canal Treatment: A Cost-effectiveness Analysis. J Endod. 2014;40:1764-70. doi: 10.1016/j.joen.2014.07.028

7. Schwendicke F, Brouwer F, Schwendicke A, Paris S. Different materials for direct pulp capping: systematic review and meta-analysis and trial sequential analysis. Clin Oral Invest. 2016;20:1121-32. doi: 10.1007/s00784 -016-1802-7

8. Paula AB, Laranjo M, Marto C-M, Paulo S, Abrantes AM, Casalta-Lopes J, et al. Direct Pulp Capping: What is the Most Effective Therapy?—Systematic Review and Meta-Analysis. J Evid Based Dent Pract. 2018;18:298-314. doi: 10.1016/j.jebdp.2018.02.002

9. Schröder U. Effects of Calcium Hydroxide-containing Pulp-capping Agents on Pulp Cell Migration, Proliferation, and Differentiation. J Dent Res. 1985;64:541-8. doi: 10.1177/002203458506400407

10. Hilton T. Keys to Clinical Success with Pulp Capping: A Review of the Literature. Oper Dent. 2009;34:615-25.

11. Qureshi A, Soujanya E, Nandakumar, Pratapkumar, Sambashivarao. Recent Advances in Pulp Capping Materials: An Overview. J Clin Diagn Res. 2014;8:316-21. doi: 10.7860/JCDR/2014/7719.3980

12. Parirokh M, Torabinejad M. Mineral Trioxide Aggregate: A Comprehensive Literature Review—Part III: Clinical Applications, Drawbacks, and Mechanism of Action. J Endod. 2010;36:400-13. doi: 10.1016/j.joen. 2009.09.009

13. Giraud T, Jeanneau C, Bergmann M, Laurent P, About I. Tricalcium Silicate Capping Materials Modulate Pulp Healing and Inflammatory Activity *in Vitro*. J Endod. 2018;44:1686-91. doi: 10.1016/j.joen.2018.06.009

14. Chen X-G, Park H-J. Chemical characteristics of O-carboxymethyl chitosans related to the preparation conditions. Carbohydr Polym. 2003;53:355-9. doi: 10.1016/S0144-8617(03)00051-1

15. Zhang H, Darvell BW. Synthesis and characterization of hydroxyapatite whiskers by hydrothermal homogeneous precipitation using acetamide. Acta Biomater. 2010;6:3216-22. doi: 10.1016/j.actbio.2010.02.011

16. Martin JJ, Riederer MS, Krebs MD, Erb RM. Understanding and overcoming shear alignment of fibers during extrusion. Soft Matter. 2015;11:400-5. doi: 10.1039/C4SM02108H

17. Liang K, Weir MD, Reynolds MA, Zhou X, Li J, Xu HHK. Poly (amido amine) and nano-calcium phosphate bonding agent to remineralize tooth dentin in cyclic artificial saliva/lactic acid. Mater Sci Eng C. 2017;72:7-17. doi: 10.1016/j.msec.2016.11.020

18. Sideridou I, Achilias DS, Spyroudi C, Karabela M. Water sorption characteristics of light-cured dental resins and composites based on Bis-EMA/PCDMA. Biomaterials. 2004;25:367-76. doi: 10.1016/S0142-9612(03)00529-5

19. Harding JL, Krebs MD. Bioinspired Deposition-Conversion Synthesis of Tunable Calcium Phosphate Coatings on Polymeric Hydrogels. ACS Biomater Sci Eng. 2017;3:2024-32. doi: 10.1021/acsbiomaterials.7b00280

20. Harding JL, Krebs MD. Controlled and Tunable Biomimetic Apatite Mineralization of Synthetic Hydrogels. Macromol Mater Eng. 2016;301:1172-80. doi: 10.1002/mame.201600151

21. Harding JL, Osmond MJ, Krebs MD. Engineering Osteoinductive Biomaterials by Bioinspired Synthesis of Apatite Coatings on Collagen Hydrogels with Varied Pore Microarchitectures. Tissue Eng Part A. 2017;23:1452-65. doi: 10.1089/ten.tea.2017.0031

22. Bacakova L, Filova E, Parizek M, Ruml T, Svorcik V. Modulation of cell adhesion, proliferation and differentiation on materials designed for body implants. Biotechnol Adv. 2011;29:739-67. doi: 10.1016/j.biotechadv.2011.06.004

23. Wang M. Developing bioactive composite materials for tissue replacement. Biomaterials. 2003;24:2133-51. doi: 10.1016/S0142-9612(03)00037-1

24. Qin W, Gao X, Ma T, Weir MD, Zou J, Song B, et al. Metformin Enhances the Differentiation of Dental Pulp Cells into Odontoblasts by Activating AMPK Signaling. J Endod. 2018;44:576-84. doi:10.1016/j.joen.2017.11.017

25. Wang S, Xia Y, Ma T, Weir MD, Ren K, Reynolds MA, et al. Novel metformin-containing resin promotes odontogenic differentiation and mineral synthesis of dental pulp stem cells. Drug Deliv and Transl Res. 2019;9:85-96. doi: 10.1007/s13346-018-00600-3

26. Lee W-H, Loo C-Y, Van KL, Zavgorodniy AV, Rohanizadeh R. Modulating protein adsorption onto hydroxyapatite particles using different amino acid treatments. J R Soc Interface. 2012;9:918-27. doi: 10.1098/rsif.2011.0586

27. Swain SK, Sarkar D. Study of BSA protein adsorption/release on hydroxyapatite nanoparticles. Appl Surf Sci. 2013;286:99-103. doi: 10.1016/j.apsusc.2013.09.027